Available online at www.sciencedirect.com
SCIENCE DIRECT
Chemical Physics 324 (2006) 236–243
Chemical Physics
www.elsevier.com/locate/chemphys

In situ measurements of oligoaniline conductance: Linking electrochemistry and molecular electronics

Fan Chen [a], Colin Nuckolls [d], Stuart Lindsay [a,b,c,*]

[a] Department of Physics and Astronomy, Arizona State University, Tempe, AZ 85287-5601, United States
[b] Department of Chemistry and Biochemistry, Arizona State University, Tempe, AZ 85287-5601, United States
[c] Biodesign Institute, Arizona State University, Tempe, AZ 85287-5601, United States
[d] Department of Chemistry, Columbia University, United States

Received 20 June 2005; accepted 28 August 2005
Available online 9 November 2005

Abstract

The single-molecule conductance of a dithiolated aniline trimer has been measured under potential control and also under an inert solvent. In each experiment, two sets of currents are found, differing by a factor 4, and these are tentatively assigned to differing connections to the electrodes (e.g., on-top vs. hollow sites). The conductances peak (to 17 ± 1.6 and 5.8 ± 0.85 nS) between the first and second oxidations of the molecule and change smoothly with surface potential. There is no evidence for a coexistence of oxidized and reduced molecules. Measurements made at a fixed surface potential as a function of tip to substrate bias show a peak current at 0.1 V followed by a region of negative differential resistance. This is accounted for semi-quantitatively by modification of the local potential by the applied bias altering the oxidation state of the molecule under the probe. Measurements made in toluene are Ohmic, indicating that the tip does not alter the oxidation state of the molecule in the absence of screening ions. We discuss the role of gap geometry and bonding in these processes.
© 2005 Elsevier B.V. All rights reserved.

Keywords: Single molecule conductance; Electrochemical gating; Molecular electronics; Oligo aniline

1. Introduction

This issue celebrates the work of Professor Noel Hush, a pioneer in adiabatic electron transfer processes [1] and a cheerleader for the emerging field of molecular electronics [2] so it seems appropriate to us to present data that helps to illustrate the connection between these two fields. It is, in some ways, remarkable that these two areas of research are not better integrated. Chemistry proceeds via electron transfer reactions that occur between molecules in solution, and molecules and electrodes in solution. The solution itself plays a key role as pointed out in the pioneering work of Marcus [3], Hush [1] and others (see, e.g., the book by Ulstrup [4]). In contrast, molecular electronic measurements are made in vacuum or other environments that are very different from ionic solutions. It is not surprising, therefore, that it is difficult to relate electrochemical data to the two-electrode potential differences at which features are seen in the characteristics of molecular electronic devices [5] (although this can be done in certain very well defined geometries [6]).

In solid state systems, local charging is dealt with in the context of the Coulomb blockade [7]. Environmentally driven electronic fluctuations, solvent screening and internal structural rearrangements are not significant, yet they are an integral part of the charge transfer process in solvated molecules (as illustrated recently by a first-principles simulation of charge transfer in DNA molecules [8]). It is now experimentally possible to measure the conductance of single molecules immersed in conducting solutions [9] and this has enabled measurement of the single-molecule conductance of an oligoaniline as a function of its oxidation state

* Corresponding author. Tel.:+ 480 965 4691.
E-mail address: Stuart.Lindsay@asu.edu (S. Lindsay).

0301-0104/$ - see front matter © 2005 Elsevier B.V. All rights reserved.
doi:10.1016/j.chemphys.2005.08.052

[10]. These measurements are made by repeatedly pushing a gold probe into a gold surface covered with dithiolated molecules and then pulling it away. As the gold junction formed between the probe and the substrate breaks, one or more molecule(s) often spans the gap, giving rise to plateaus of constant current as the gold elongates but the overall conductance is dominated by the molecule [11–13].

Our first study of an oligoaniline under potential control [10] produced several novel findings: (a) The molecular conductance peaked after the first oxidation of the oligoaniline, but the peak conductance (6 nS) was much less than the metallic conductance (equivalent to 77 μS for a single molecule) observed in bulk polyaniline. (b) The current–voltage characteristics in a non-conducting solvent (toluene) was linear at low bias (<0.5 V). (c) The current voltage characteristic changed completely when the molecule was held under potential control in 50 mM H_2SO_4. The current peaked at 0.1 V, then fell rapidly with increasing bias. Such low-bias negative differential resistance (NDR) has not been observed before. It was accounted for semi-quantitatively by taking account of the modification of the local potential by the applied tip–substrate bias. This results in reduction of previously oxidized molecules as the probe is made more negative, switching the molecule back to its less-conductive form. Just as importantly, the lack of features in the current–voltage characteristics obtained in toluene illustrates the role of the ions in stabilizing charge transfer (in this case both in screening charge states and in stabilizing the conductive salt [14]). (d) Current–voltage characteristics obtained by sweeping the bias applied to single molecules (as opposed to the point-by-point averaging of data for hundreds of single molecules) shown large molecule to molecule variations that were repeatable *for a given molecule.* From this we conclude that *variations in the local fixed geometry of the gap influence the electronic properties of the molecules.*

This prior work was carried out with an 8-benzene-ring oligomer (containing 7 nitrogen atoms). We have now completed a study of a shorter oligomer (containing 4 rings and 3 nitrogen atoms). Broadly, this new study confirms the results reported for the longer oligomer [10]. However, we have observed a new feature of the STM breakjunction method used to obtain these data. This is the observation of more than one molecular conductance state, possibly a reflection of distinctly different molecular attachment geometries. We also take advantage of this longer report to expand our description of the experimental method and to discuss these results in a broader context.

2. Experimental methods

2.1. Synthesis of the samples

The synthesis of the aniline core was accomplished by a method recently developed by Buchwald and coworkers [14] that utilizes mild, palladium-based cross-coupling reactions. The aniline core could be synthesized in a number of lengths and was protected from oxidation by blocking the nitrogens with a *t*-butyl carbamate (Boc) group (an alternative method based on methylated nitrogens was described earlier by Flatt and Tour [15]). End-capping groups were coupled onto this core. These groups were terminated in thiols blocked with an ethyl-TMS group [16]. The final step of the synthesis was to exchange the sulfur protecting groups for the more common thiol acetates [17] and to remove the Boc protecting group by thermolysis under inert atmosphere. For the present work, we synthesized the dithioacetate trimer **1** shown below.

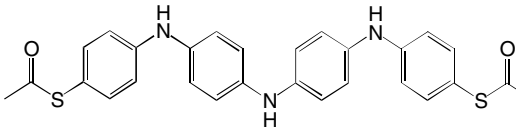

1

2.2. Preparation of monolayers

Immediately after removal of the Boc groups, oligomers were dissolved in freshly distilled, argon-sparged *N*,*N*-dimethylformamide, DMF, to a final concentration of 30 μg/ml (as determined by UV–visible spectrophotometry [14]). An Au substrate [18] was annealed with a hydrogen flame and submerged in 20 ml of this solution. 30 μl of concentrated NH_4OH was added (to deprotect the end groups [19]) and the solution left in contact with the substrate for 3 h under an Ar atmosphere. The substrates were then copiously rinsed with DMF, methanol and DI water.

2.3. Characterization of monolayers

Functionalized substrates were characterized by FTIR, cyclic voltammetry (see below) and STM imaging. Reflectance FTIR spectra (Bruker IFS 66 V/S) taken from substrates used in the conductance measurements were similar to those reported for polyaniline [20]. STM images are consistent with a disordered sub-monolayer coverage.

2.4. Cyclic voltammetry

We have previously studied the cyclic voltammetry of the dithioacetate heptamer on an ITO electrode in order to compare to the voltamettry obtained for a phenyl-capped heptamer studied by Sadighi et al. [14] (as described in the online supporting information for the paper by Chen et al. [10]). The different terminae result in only a small shift (ca. 80 mV) of the first and second oxidation peaks. Our STM cell uses an Ag wire quasi reference and this was calibrated against an Ag/AgCl reference electrode using both ferrocene and gold oxidation peaks. The Ag wire scale is shifted down from Ag/AgCl by 0.3 V (for pH < 4) so that the first hepta-aniline oxidation peak occurs at ca. 0.18 V on this scale [10]. The quasi reference was stable to within

about 20 mV from run to run with a given chemistry. The prominent features in the voltammograms change only for oligomers smaller than ca. 5 aromatic rings [14] with the oxidation potential increasing by about 0.2 V for the trimer [21]. The voltammogram for the monolayer of the trimer on Au(1 1 1) obtained in 50 mM H_2SO_4 (see Fig. 4(a)) shows the first oxidation at ca. 0.33 V (0.15 V above its location in the hepta aniline, consistent, within uncertainties in the reference scale [10], with the expected increase [21]). The second oxidation at ca. 0.75 V is shifted about 0.13 V positive of its position in hepta-aniline. The second peak is not reversible and potentials above 0.65 V were avoided when electronic data were collected.

2.5. STM measurements

The STM was performed with a PicoSTM system (Molecular Imaging, Tempe). Probes were formed by cutting a 0.25 mm diameter Au (99.999%) wire and insulating it with Apiezon wax [22]. Ag wire and Pt wires were used for the reference and counter electrodes, respectively. They were cleaned in acetone, methanol and DI water and dried in an N_2 stream. The Teflon® liquid cell was cleaned with piranha (3:1 H_2SO_4/H_2O_2, v/v) and then refluxed with methanol/dichloromethane in a Soxhlet extractor.

Caution. Piranha solution is a very strong oxidant and is extremely dangerous to work with; gloves, goggles, and a face shield should be worn.

The aniline trimer coated Au substrate was placed on the microscope and covered with Ar-sparged 0.05 M H_2SO_4. The first oxidation peak was verified by cyclic voltammetry carried out with the microscope's built-in potentiostat and the sample then set to the desired surface potential. The entire liquid cell was enclosed by a sealed chamber that was flushed with Ar. The surface was first imaged to ensure that a clean sub-monolayer was present, and current measurements made at a fixed tip–substrate bias as a function of time as the tip is withdrawn after hard contact with the surface [11]. Data were acquired with a digital oscilloscope interfaced to a Labview data acquisition card, using a breakout box to interface with the PicoSTM. Measurements in freshly distilled toluene were made with a bare Au probe cleaned in ethanol, rinsed in DI water and blown dry with argon. The samples were maintained under an argon environment during measurement.

Measurements made under potential control were taken repeated several times, meaning that some were taken after the sample potential had been as high as 0.65 V and some were taken approached from lower potentials. The data were reproducible (within the scatter shown). Data for single molecules taken as the potential is swept is given in the paper by Chen et al. [10].

2.6. Data analysis

Selection of data and its subsequent analysis are critical aspects of the procedure hitherto not discussed in detail.

(a) *Selection of data*. The STM breakjunction method is subject to many artifacts, not least because particles of contamination in the gap will give rise to non-reproducible curves. With clean probes, as many as 80% of the pulls are usable [13]. However, the coating required for electrochemical operation [22] contaminates the probes and reduces this fraction to around 20%. Examples of 'good' curves are given in Fig. 1(a). The current fall-off before and after each current plateau is on the order of a factor 10 per angstrom (when the time data are converted to distance using the known velocity of the probe). This is consistent with the gold work function (of 5.3 eV) and provides one criterion for picking 'good' curves [13]. Examples of rejected curves are given in Fig. 1(b). Curve 1 decays rapidly but shows no features. Such curves are rejected because they contribute to a spurious peak near zero current. Curve 2 is obviously noisy. Curve 3 appears to have steps in it, but close inspection shows that they are periodic, owing to oscillatory electrical noise and with a lack of bias dependence for features of this particular current separation. Curves 4 and 5 are examples of possible steps that fail to meet the current decay criterion in the regions that border the steps.

(b) *Forming the current histograms*. A Labview program was written to analyze the selected current–time curves automatically to give results such as those shown in Fig. 2. Each individual curve is first converted to a current histogram using 200 bins/nA. Current steps correspond to regions of relatively constant current and show up as peaks in this histogram. There are also large spurious peaks at zero bias (owing to the tails of the pulling curves [13]) and at the saturation current of the current to voltage converter. A window of 20 bins in width is then slid over the histogram starting from zero current. If the difference between the maximum and the minimum current values in the window exceed a user-set threshold – 20 counts in this case – and the maximum occurs in the center of the window, then a unit count is assigned to the position of the center of the window at which the conditions were fulfilled. This procedure rejects the spurious peaks at zero current and the saturation current (because the maximum is never in the middle of the window). The process is repeated for

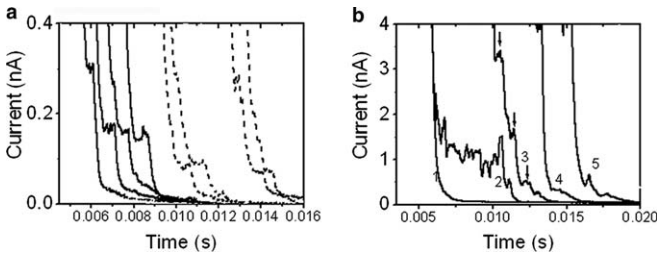

Fig. 1. Current vs. distance data for the STM breakjunctions experiments (data are shown for a tip–substrate bias of 50 mV at a surface potential of 0.3 V vs. Ag). (a) Examples of good curves – solid lines show high current steps and dashed lines show low current steps. (b) Examples of rejected data (discussed in the text).

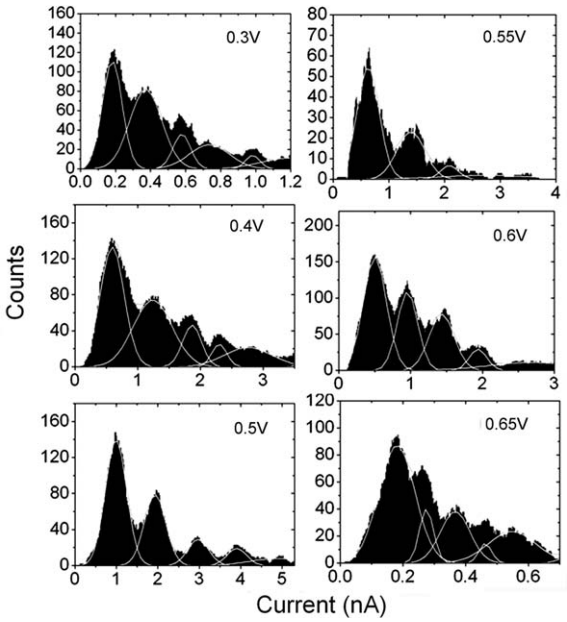

Fig. 2. Histograms of current recorded in curves like those shown in Fig. 1a. The data here are for a tip–substrate bias of 50 mV at the surface potentials shown in the upper right hand corner of each panel. The histograms were compiled from high-current steps only. The white lines are Gaussian fits to each peak.

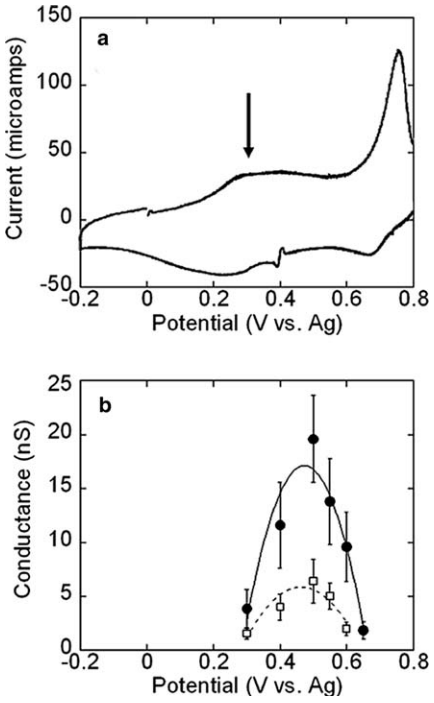

Fig. 3. (a) Voltammogram for a monolayer of the dithiol aniline trimer on Au(1 1 1) in 50 mM H_2SO_4. The arrow points to the first oxidation peak at ca. 0.33 V vs an Ag quasi reference. (b) Single molecule conductance for the high current series (black dots) and the low current series (open squares) as a function of the surface potential. The lines are fits to a quadratic dependence of conductance on surface potential. Error bars are the half-width of the first peaks in the histograms.

all accepted curves and a histogram of the unit-counts compiled. Examples are shown in Fig. 2.

In the present work, we encountered more than one series of peaks. We have analyzed a similar problem in the case of octanedithiol using a logarithmic current to voltage converter, and concluding that the multiple current values probably arise from different attachment geometries [13]. In that work, we analyzed compound histograms that contained data for both sets of peaks. Here, we separated the data after the histogram analysis of the individual curves. Based on a study of the compound histogram, the unit counts were assigned to high current steps or low current steps. The series shown in Fig. 2 are for the high current steps. A similar series of histograms (but with more variable peak widths) was found for the low current steps (data not shown).

3. Results

3.1. Data obtained at constant probe bias as a function of substrate potential

Examples of good curves showing high steps (solid lines) and low steps (dashed lines) are shown in Fig. 1(a). In the first experiment, we applied a constant tip to substrate bias of 50 mV (the tip was negative with respect to the substrate which was held under potential control) and took data as a function of the substrate surface potential. The histograms (Fig. 2) correspond to the data obtained at each surface potential (listed vs. Ag.). The voltammogram for the trimer on Au(1 1 1) in 50 mM H_2SO_4 is shown in Fig. 3(a) (the arrow points to the approximate half-wave potential for the first redox process at ca. 0.3 V vs. Ag). The conductances obtained from the current histograms for both the high steps (Fig. 2) and the low steps (histograms not shown) are plotted as a function of potential in Fig. 3(b). The error bars are estimated from the half-widths of the first histogram peak. Each series shows a peak conductance near 0.5 V vs. Ag. The conductances can be fitted by a quadratic dependence on surface potential, E_S:

$$G = G_{max} - k(E_S - E_S^M)^2, \quad (1)$$

where G_{max} is the peak conductance and is the potential at which peak conductance is observed. The fitting parameters for both sets of data are listed in Table 1.

3.2. Data obtained as a function of tip to substrate bias in toluene

Again, two sets of current data were found for this molecule in this experiment, and the current–voltage data extracted from them are shown in Fig. 4. The characteristics

Table 1
Parameters for the quadratic fit to the dependence of the single-molecule conductance on potential

	G_{max} (nS)	k (S/V^2)	E_S^M (V vs. Ag)
High current series	17 ± 1.6	475 ± 83	0.47 ± 0.01
Low current series	5.8 ± 0.85	176 ± 57	0.46 ± 0.02

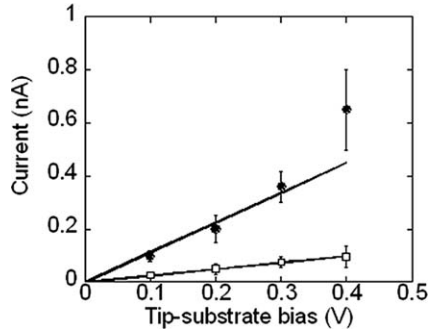

Fig. 4. Current–voltage characteristics for the dithiol aniline trimer in toluene. Black dots are for the high current steps and open squares are for the low current steps. The ratio of the frequency of occurrence of high current features to that of low current features in the data was 1.3:1 with a standard deviation of 0.13 across the bias range. The lines are linear fits to the low bias region.

are well fitted by an Ohmic response (0–0.3 V for the high current series and 0–0.4 V for the low current series) yielding conductances of 1.13 ± 0.06 and 0.25 ± 0.005 nS, a ratio of 4.5:1 between the conductance of the high current and the low current configurations for the low bias region. The high current series shows a significant departure from linearity at higher bias, not observed in the case of hepta aniline [10].

3.3. Data obtained as a function of tip–substrate bias at constant surface potential

Data were obtained with the substrate held at 0.6 V vs. Ag in 50 mM H_2SO_4 for tip biases between 0 and 0.4 V (pulling curves became noisy at higher bias). Fewer data points were obtained than was the case for the hepta aniline [10] because of the added burden of analyzing data for both the high and low current series. Nonetheless, an NDR peak is observed just as in the case of hepta aniline (Fig. 5). Assuming that the local potential under the tip is modified by a term αV_{ts} where V_{ts} is the tip–substrate bias and α is a geometrical constant (see discussion below), we can use Eq. (1) for the conductance to obtain the following expression for the current:

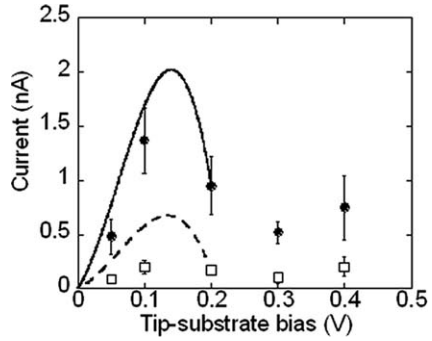

Fig. 5. Current–voltage curves for a fixed surface potential of 0.6 V vs. Ag in 50 mM H_2SO_4. The black dots are data for the high current series and the open squares are for the low current series. The lines are fits using Eq. (2).

$$i = GV_{ts} = \left(G_{max} - k(E_S - E_S^M - \alpha V_{ts})^2\right) V_{ts}. \quad (2)$$

Here, the sign convention is that V_{ts} is positive if it opposes the substrate field. That is to say, if the substrate is held at a positive potential with respect to the reference electrode, a positive V_{ts} means that the tip is biased negative with respect to the substrate, lowering the local electric field in the gap. Here, $E_S = 0.6$ V and the values of the other parameters are taken from Table 1. The solid curve is a fit to the three lowest bias high current data points with $\alpha = 1.44 \pm 0.04$ and the dashed curve is a fit to the three lowest bias low current data points with $\alpha = 1.5 \pm 0.1$.

4. Discussion

4.1. Observation of two sets of current data

The novel feature of the data obtained with this shorter oligomer is the observation of two sets of current data. Averaged over all the measurements presented here, the ratio between the low and high current series is roughly constant at $4.4 \pm$ 1:1. It is reasonably consistent across the experiments: for example it is 5.3:1 at 50 mV bias at a potential of 0.6 V vs. Ag for the data shown in Fig. 5 and 4.9:1 in the same conditions for the data shown in Fig. 3. This ratio is similar to what was observed in the case of octanedithiol (4:1) [13]. In that case, the spurious formation of dimers could be ruled out as a source of the low current data using the known value of the current decay constant, β. We have shown elsewhere that this 4:1 ratio is about the factor to be expected when different bonding geometries are compared, specifically hollow site vs. on-top [13]. The ratio appears to be somewhat enhanced for more conductive molecules. For example, it is clearly higher for the 0.4V data in toluene where the current has started to rise above the linear response. A similar effect is seen in simulations, where, for example, the ratio is higher for a highly conducting form of a switchable photochromic molecule [13]. This dependence on conductance shows that the effects of contacts cannot be isolated from the properties of the molecule, since, in addition to altering electronic transparency, different contact also change the relative energy alignment of the Fermi level (O.F. Sankey, personal communication). The effect also appears to be more pronounced for shorter molecules (the aniline trimer, octanedithiol) and it has not been observed in longer molecules (the aniline heptamer and a series of carotenoids [23]). Two possible explanations are that (1) the effect of contacts is less significant in longer molecules or (2) the smaller current series lies below the noise level in longer molecules.

4.2. Dependence of the molecular conductance on surface potential

Our results are broadly similar to what was observed for the hepta aniline, with the conductance peaking sharply at a potential somewhat above the first oxidation peak. This behavior is expected on the basis of the macroscopic prop-

erties of polyaniline which turns metallic on oxidation to the emeraldine salt, becoming insulating again on a second oxidation step to the perigraniline form [24,25]. It may, however, be a quite general property of molecules that become oxidized while in a tunnel junction [26,27]. To begin with, oxidation generates a partially filled HOMO that would give a long oligomer a metallic character were it not for Pierls-distortions [25]. Secondly, the charged state can be quite delocalized [28] possibly giving rise to enhanced overlap with the metal contacts. Thirdly, the presence of a redox active molecule in the gap opens up a number of channels for extra current [27]. The details of the process depend upon the strength of coupling between the molecule and electrodes, the local electric field at the molecule as well as the overpotential and exact location of levels with respect to the Fermi level of the contacts [27]. Two simple limits can be considered. In the weak-coupling limit where transport occurs with charging and relaxation of the molecule, followed by discharging to the second electrode, the current is maximum at the half-wave potential where the overlap between the density of reduced and oxidized states is highest [26,27,29]. Referring to Fig. 3(a), the oxidation wave peaks at about 0.33 V and the reduction wave peaks at about 0.23 V putting the half-wave potential, E_0, at about 0.3 V vs. Ag, clearly significantly below the conductance peak at ca. 0.5 V. In the strong-coupling limit, the electrons tunnel through the unoccupied levels of the oxidized molecule, giving rise to a peak conductance at $E_0 + \lambda$ where λ is the reorganization energy [26]. Interpreted this way, these data would imply that $\lambda \approx 0.2$ eV (but see below).

The distributions of current as a function of potential are also revealing. The half-wave potential is usually thought of as the point where equal numbers of molecules are in the reduced and oxidized forms, with an increasing number in, e.g., the oxidized form as the overpotential is increased. Yet it is clear that the electronic properties of the molecules evolve smoothly with overpotential; both the high and low current data change continuously. One possibility is that individual molecules fluctuate between oxidized and reduced states at a speed that is to high to lead to observable fluctuations in the currents measured here. Nonetheless, the conductance would then reflect the relative amounts of time the molecules spent in the two states. In particular, one can eliminate the possibility that the more highly charged molecules 'burn out' (e.g., through reactions with oxygen [30]) because the conductance decreases smoothly as the surface potential is increased to approach the second oxidation step. To see this, suppose that the oxidized molecules maintained a (constant) high conductivity at potentials where the entire population was oxidized. Then 'burn out' on increasing the potential would cause two populations of molecule to be found: Molecules with high (and constant) conductance and 'burnt out' molecules with lower (perhaps unmeasurable) conductivities. The smooth transition implies that the state of individual molecule is changing with potential as the second oxidation is approached. Once again, it is possible that individual molecules are stochastically switching between oxidation states, but at a rate that is to fast to be detected in these experiments.

4.3. Negative differential resistance and alteration of the local potential by the applied bias

The present data replicate the phenomenon of low bias NDR first observed in the hepta aniline oligomer [10] and are semiquantitatively accounted for with a very simple model that takes account of the modification of the local potential by the tip–substrate electric field. The constant α reflects the influence of tip–substrate bias relative to the double-layer field and the values found here (1.44 ± 0.04 and $\alpha = 1.5 \pm 0.1$) agree well with the value found for the hepta aniline oligomer [10] (1.4 ± 0.03 – confirmed with a series of measurements at different surface potentials [10]). A value of $\alpha > 1$ implies that the tip bias influences the molecule more than the double-layer field (expressed in terms of volts relative to a reference electrode). This may just reflect a diminuation of the effect of potential control in the gap. Previous measurements of polyaniline grown in a nm-scale gap did not show NDR (though the current falls off at higher bias suggesting the possibility of NDR at yet higher bias [31]). However, the polyaniline filaments were not covalently bonded to each electrode in that work [31], raising the possibility that the potential drop across the molecule itself is smaller than in the present work where the molecule is covalently connected to each contact.

4.4. Environment and molecular charging

The dramatic difference between the current–voltage characteristics in toluene (Fig. 4) and under potential control in H_2SO_4 (Fig. 5) illustrates the influence of the environment on the electronic properties of the molecule. The charge-state of the molecule remains unaltered as the tip–substrate bias is swept up to 0.4 V, whereas the charge state is perturbed by application of 0.1 V when the molecule is in electrolyte. It is interesting to note that the shorter molecule shows some sign of non-linearity in its *IV* characteristic taken in toluene (high current series in Fig. 4). This might reflect an effect of contact geometry on the alignment of molecular levels with respect to the Fermi energy of the metal.

Note that although data are shown here for only one direction of bias, the effect on charging of the molecule will be symmetrical if neither the tip not substrate are held under potential control [27]. This difference with change of environment illustrates the critical role of the environmental polarizability in charge transfer. Thus, comparison of electrochemical data with molecular electronic data require more than a relationship between reference potentials and workfunctions [32] because the role of the solvent in screening the charged state is critical [30].

4.5. Effects of attachment geometry

In a very elegant series of series of experiments, Hipps and coworkers have shown how the potential for peak tunneling current coincides with the half-wave potential when data are presented relative to the vacuum energy [6]. These results serve to illustrate the importance of two factors. The first is the role of screening and the second is the role of the potential distribution in the gap. In these experiments, planar molecules are physisorbed onto clean metal surfaces and the molecule is assumed to be at the potential of the substrate (which will be true if the adsorption dipole is small). The amount of charging and relaxation of the molecules is not known. One might expect that it would be small in this case of tight coupling to a metal substrate, and this, in turn, implies that the reorganization energy, λ, is also small, since, in this limit, the peak current should occur at $E_0 + \lambda$. This is probably reasonable. Taking the classical expression for outer-shell reorganization for a molecule on an electrode [3]

$$\lambda \approx \frac{e}{2\varepsilon_0}\left(\frac{1}{\varepsilon_\infty} - \frac{1}{\varepsilon_s}\right)\left(\frac{1}{a} - \frac{1}{2d}\right) \text{ eV}, \tag{3}$$

where ε_0, ε_∞ and ε_s are the dielectric constants of free space, the medium at high frequency and the medium at low frequency, respectively. a is the ionic radius and $2d$ is the distance to the image charge in the electrode. In the geometries studied by Hipps, $a \approx 2d$ so λ will be small (the electrode provides the screening charge to stabilize the ion). If, however, the charged species is some distance from the electrode, the image charge contribution will be smaller and ions will play a more significant role (as in the present work).

The second important factor that depends on local geometry and bonding is the potential at the molecule. The attachment geometry used in the UHV experiments of Hipps and coworkers [6] permitted the use of the simplifying assumption that the metal substrate and adsorbed molecule were at approximately the same potential. In the present experiments, the strong influence of the probe potential suggests that the molecular potential lies somewhere between that of the tip and the substrate (but the measurements made at low tip to substrate bias probably yield a reasonable estimate for λ because of the built in reference to the half-wave potential of the adsorbed molecules).

It is much harder to interpret data taken with no potential control and less well-defined contacts. Thus, estimates of the half-wave potential for the process $Fe^{++} \Longleftrightarrow Fe^{+++}$ relative to the Au Fermi level suggest that the process should occur at a few tenths of a volt whereas it appears that it occurs at a bias of ca. 1.5 V in a two electrode geometry [30,33]. Assuming that the process in that case really is the oxidation to ferricenium, then there is a significant potential drop between the electrodes and the molecule and/or charging energy is raised significantly in the absence of screening ions.

We have not taken advantage of a comparison of the present data with our earlier results for hepta-aniline to try to extract values for the electronic decay constant in the neutral and oxidized forms of oligoaniline. This would be a very interesting exercise, but it requires measurements of at least one more length of oligomer, both to test the length-dependence of the decay, and to avoid ambiguities associated with the multiple current values observed in this shorter oligomer.

Acknowledgements

This work was supported by the National Science Foundation through NIRT (ECS01101175) and NSEC (CHE-0117752) awards and the New York State Office of Science, Technology, and Academic Research. We thank Nongjian Tao, Kerry Hipps and Jin He for useful discussions.

References

[1] N.S. Hush, J. Electroanal. Chem. 470 (1999) 170.
[2] N.S. Hush, Ann. N.Y. Acad. Sci. 1006 (2003) 1.
[3] R.A. Marcus, J. Phys. Chem. 43 (1965) 679.
[4] J. Ulstrup, Charge Transfer Processes in Condensed Media, Springer-Verlag, Berlin, 1979.
[5] S. Kubatkin, A. Danilov, M. Hjort, J. Cornil, J.-L. Bredas, N. Stuhr-Hansen, P. Hedegard, T. Bjornholm, Nature 425 (2003) 698.
[6] K.W. Hipps, in: Handbook of Applied Solid State Spectroscopy, Kluwer, Berlin, in press.
[7] G. Fagas, K. Richter, Introducing Molecular Electronics, Springer, Berlin, 2005.
[8] R.N. Barnett, C.L. Cleveland, A. Joy, U. Landman, G.B. Schuster, Science 294 (2001) 567.
[9] W. Haiss, H. van Zalinge, S.J. Higgins, D. Bethell, H. Hobenreich, D.J. Schiffrin, R.J. Nichols, J. Am. Chem. Soc. 125 (2003) 15294; B. Xu, P.M. Zhang, X.L. Li, N.J. Tao, Nanoletts 4 (2004) 1105.
[10] F. Chen, J. He, C. Nuckolls, T. Roberts, J. Klare, S.M. Lindsay, NanoLetters 5 (2005) 503.
[11] B. Xu, N.J. Tao, Science 301 (2003) 1221.
[12] B. Xu, X. Xiao, N.J. Tao, J. Am. Chem. Soc. 125 (2003) 16164.
[13] J. He, S.M. Lindsay, N.J. Tao, X. Li, Faraday Discussions 131, in press.
[14] J.P. Sadighi, R.A. Singer, S.L. Buchwald, J. Am. Chem. Soc. 120 (1998) 4960.
[15] A.K. Flatt, J.M. Tour, Tetrahedron Lett. 44 (2003) 6699.
[16] S.K. Pollack, J. Naciri, J. Mastrangelo, C.H. Patterson, J. Torres, M. Moore, R. Shashidhar, J.G. Kushmerick, Langmuir 20 (5) (2004) 1838; C.J. Yu, Y. Chong, J.F. Kayyem, M. Gozin, J. Org. Chem. 64 (6) (1999) 2070.
[17] L. Jones III, J.S. Schumm, J.M. Tour, J. Org. Chem. 62 (5) (1997) 1388; D.L. Pearson, J.M. Tour, J. Org. Chem. 62 (5) (1997) 1376; J.M. Tour, L. Jones II, D.L. Pearson, J.J.S. Lamba, T.P. Burgin, G.M. Whitesides, D.L. Allara, A.N. Parikh, S. Atre, J. Am. Chem. Soc. 117 (37) (1995) 9529.
[18] J.A. DeRose, T. Thundat, L.A. Nagahara, S.M. Lindsay, Surf. Sci. 256 (1991) 102.
[19] L. Cai, Y. Yao, J. Yang, D.W. Price, J.M. Tour, Chem. Mater. 14 (2002) 2905.
[20] C.J. Mathai, S. Saravanan, M.R. Anantharaman, S. Venkitachalam, S. Jayalekshmi, J. Phys. D: Appl. Phys. 35 (2002) 2206; F. Wudl, R.O. Angus, F.L. Lu, P.M. Allemand, D.J. Vachon, M. Nowak, Z.X. Liu, A.J. Heeger, J. Am. Chem. Soc. 109 (1987) 3677.
[21] J. Honzl, M. Tlustakova, J. Polym. Sci. C22 (1968) 451.
[22] L.A. Nagahara, T. Thundat, S.M. Lindsay, Rev. Sci. Instrum. 60 (1989) 3128.

[23] J. He, F. Chen, J. Li, O.F. Sankey, Y. Terazono, C. Herrero, D. Gust, T.A. Moore, A.L. Moore, S.M. Lindsay, J. Am. Chem. Soc. Commun. 127 (2005) 1384.
[24] D. Ofer, R.M. Crooks, M.S. Wrighton, J. Am. Chem. Soc. 112 (1990) 7869;
W. Liang, M.P. Shores, M. Bockrath, J.R. Long, H. Park, Nature 417 (2002) 725;
J. Park, A.N. Pasupathy, J.I. Goldsmith, C. Chang, Y. Yaish, J.R. Petta, M. Rinkoski, J.P. Sethna, H.D. Abruna, P.L. McEuen, D.C. Ralph, Nature 417 (2002) 722.
[25] J.L. Bredas, in: W.R. Salaneck, I. Lundström, B. Rånby (Eds.), Conjugated Polymers and Related Materials: Proceedings of the 1991 Nobel Symposium in Chemistry, Oxford University Press, Oxford, 1993, p. 187.
[26] W. Schmickler, J. Electroanal. Chem. Interfacial Electrochem. 296 (1990) 283.
[27] J. Zhang, Q. Chi, A.M. Kuznetsov, A.G. Hansen, H. Wackerbarth, H.E.M. Christensen, J.E.T. Andersen, J. Ulstrup, J. Phys. Chem. B 106 (2002) 1131.
[28] J.-L. Bredas, G.B. Street, Acc. Chem. Res. 18 (1985) 309.
[29] W. Schmickler, Interfacial Electrochemistry, Oxford University Press, Oxford, 1996.
[30] J. He, S. Lindsay, J. Am. Chem. Soc. 127 (2005) 11932–11933.
[31] H. He, X.J.S. Zhu, N.J. Tao, J. Appl. Phys. 78 (2001) 811.
[32] D.M. Kolb, Zeischrift Fur Physikalische Chemie Neue Folge Bd 154S (1987) 179.
[33] C.B. Gorman, R.L. Carroll, R.R. Fuierer, Langmuir 17 (22) (2001) 6923.